THE ASTROPHYSICAL JOURNAL, 361:607–620, 1990 October 1

TERMINAL VELOCITIES FOR A LARGE SAMPLE OF O STARS, B SUPERGIANTS, AND WOLF-RAYET STARS

RAMAN K. PRINJA AND M. J. BARLOW
Department of Physics and Astronomy, University College London
AND
IAN D. HOWARTH[1]
Joint Institute for Laboratory Astrophysics, University of Colorado, and National Institute of Standards and Technology
Received 1989 November 13; accepted 1990 April 2

ABSTRACT

We argue that easily measured, reliable estimates of terminal velocities for early-type stars are provided (1) by the central velocity asymptotically approached by narrow absorption features and (2) by the violet limit of zero residual intensity in saturated P Cygni profiles. We use these estimators to determine terminal velocities, v_∞, for 181 O stars, 70 early B supergiants, and 35 Wolf-Rayet stars. For OB stars our values are typically 15%–20% smaller than the extreme violet edge velocities, v_{edge}, while for WR stars $v_\infty = 0.76 v_{edge}$ on average. We give new mass-loss rates for WR stars which are thermal radio emitters, taking into account our new terminal velocities and recent revisions to estimates of distances and to the mean nuclear mass per electron. We examine the relationships between v_∞, the surface escape velocities, and effective temperatures.

Subject headings: stars: early-type — stars: winds — stars: Wolf-Rayet

I. INTRODUCTION

The terminal velocity of a stellar wind, v_∞, is defined as the velocity of outflowing matter at large distances from the star, where it is no longer experiencing significant acceleration but is not yet interacting significantly with the interstellar medium. Reliable estimates of v_∞ are needed for several reasons. The theory of radiation pressure–driven winds makes important predictions concerning the relationship between the terminal velocity and the photospheric escape velocity (Abbott 1978). Terminal velocities are needed for the determination of mass-loss rates, $\dot{M}$, derived, for example, from modeling UV resonance line profiles (where $\dot{M} \propto v_\infty^2$) or from radio measurements of the free-free radiation from the winds ($\dot{M} \propto v_\infty$). Knowledge of wind terminal velocities is also needed for the application of theories for the interaction between stellar winds and the interstellar medium.

Since the time of the first large-scale ultraviolet spectroscopic survey of the mass-loss characteristics of luminous OB stars (Snow and Morton 1976), the terminal velocity of a stellar wind has normally been observationally defined as the modulus of the largest negative velocity seen in absorption in the P Cygni profiles of UV resonance lines. Examples of this blue absorption edge velocity are shown in Figure 1. (We use v_{edge} to signify the edge velocity observed in a given line and v_{max} to denote the maximum edge velocity in any line.) However, even presuming that the optical depth in the line is sufficient for it to be detectable at large radii, this operational definition will be correct only if there are *no* significant line broadening mechanisms other than the macroscopic Doppler broadening brought about by the bulk velocity field. The observation of P Cygni profiles showing extended regions of zero residual intensity and blue wings with finite width throw the applicability of this condition into question.

Models of saturated P Cygni profiles using the Sobolev approximation and incorporating velocity laws which increase monotonically with radius (e.g., Castor and Lamers 1979) predict that zero intensity should be reached only at v_∞ and that the profiles should return sharply to unit continuum intensity (since the forward-scattering halo contains material at all projected line of sight velocities up to, but excluding, the terminal velocity). Observed saturated profiles instead often show an extended absorption region which is black, i.e., has zero residual intensity within observational uncertainties, while a finite absorption region between the shortward edge of the black absorption core (v_{black}) and the velocity v_{edge} at which the profile intersects the continuum level is normal (see Fig. 1). These effects are consistent with nonmonotonic wind velocity laws, as first shown by Hamann (1980, 1981), who parameterized the required local velocity fields by large random microturbulent motions, and by Lucy (1982, 1983), who adopted large numbers of forward-propagating shocks resulting from instabilities in the flows as a specific physical model. The recent numerical modelling of radiatively driven non-laminar stellar winds by Owocki, Castor and Rybicki (1988, hereafter OCR) predicts that *reverse* shocks in the flow should lead to the highest velocity material being located in rarefaction zones, so that the small amount of material with velocities much higher than the terminal flow speed should cause a residual amount of absorption on the blue edge. An implication of Lucy's model (and of OCR's, but in the context of a more realistic physical structure) is that v_{max} can exceed v_∞ by an amount related to the amplitude of shocks in the wind, and thus, as discussed by Abbott (1985), v_{black} should provide a better estimate of the wind terminal velocity than does v_{max}.

In addition to these effects, discrete absorption components are commonly found within the absorption troughs of unsaturated P Cygni resonance line profiles seen in the UV spectra of luminous OB stars, occurring at the same velocity in different ions (Morton 1976; Snow 1977; Lamers, Gathier, and Snow 1982; Prinja and Howarth 1986). Howarth and Prinja (1989) have shown that the available data are consistent with the hypothesis that the mechanism responsible for discrete com-

[1] 1988–1989 JILA Visiting Fellow.

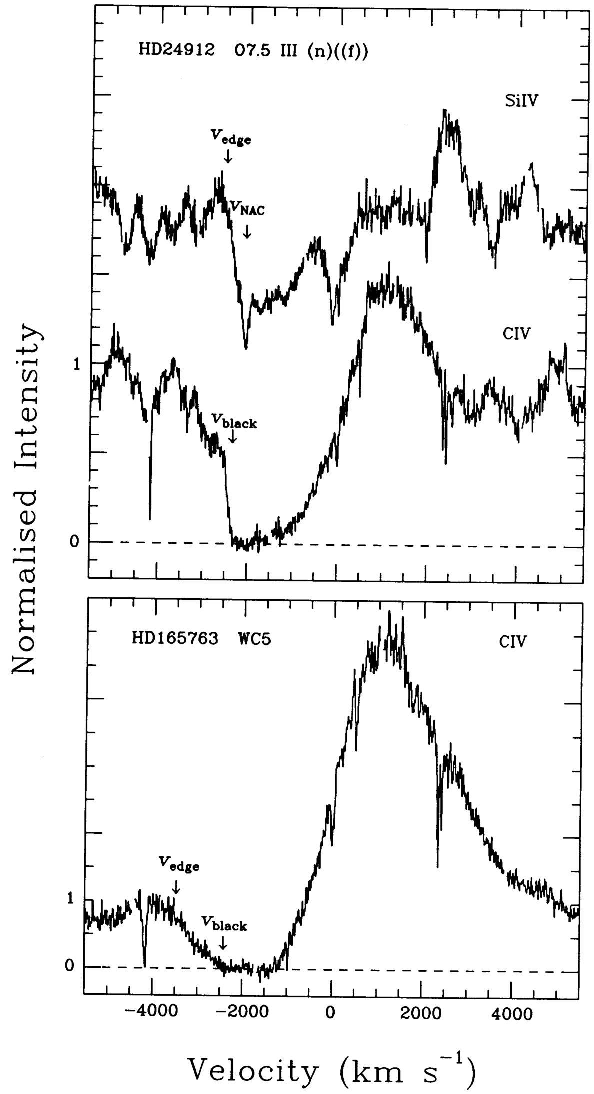

FIG. 1.—Examples of the principal stellar wind velocity measurements made on the UV resonance line profiles of O and WR stars.

ponents operates in *all* O stars. An example of discrete absorption features in the Si IV spectrum of HD 24912 is shown in Figure 1.

Recent investigations of short-term (hours–days) variability in the UV P Cygni profiles of selected O stars have shown that the velocities of discrete absorption components have a systematic time dependence (Prinja, Howarth, and Henrichs 1987; Prinja 1988; Prinja and Howarth 1988). These studies show that the discrete components first appear as broad optical depth enhancements ($\Delta v \simeq 0.5 v_{max}$) at $\sim 0.5 v_{max}$ and evolve into high-velocity narrow absorption components (NACs; $\Delta v_{NAC} \simeq 0.1 v_{max}$) with central velocities v_{NAC} which asymptotically approach $\sim 0.85 v_{max}$ (Howarth and Prinja 1989). The time scale for this velocity evolution appears to be proportional to the rotation period of the star (Prinja 1988). While more than one set of discrete absorption components may be visible in the spectrum of a star at any one time, a single "snapshot" UV spectrum will usually show a narrow absorption component at $v_{NAC} \sim 0.8 v_{max}$. It has been proposed by Prinja and Howarth (1986), by Henrichs, Kaper, and Zwarthoed (1988), and by Howarth and Prinja (1989) that the final central velocity of the discrete absorption components, $v_{NAC}(t \to \infty)$, also provides a better indicator of v_∞ than does v_{max}.

In this paper we will argue that measurements of both black absorption edge velocities and of narrow absorption component velocities give consistent estimates of wind terminal velocities and that either diagnostic may be used in isolation in a straightforward manner to estimate v_∞. Using high-resolution *IUE* spectra, we then go on to measure wind terminal velocities for 181 O stars, for 70 B0–B3 supergiants, and for 35 Wolf-Rayet (WR) stars.

II. OBSERVATIONAL INDICATORS OF v_∞

The discrete absorption components observed in unsaturated P Cygni profiles represent an optical depth enhancement at some specific velocity in the wind, associated with material having a finite velocity dispersion. We interpret the maximum velocity of these features (the narrow components) as the terminal velocity, with the difference $v_{edge} - v_\infty$ arising from a *local* velocity field, which has been parameterized as "microturbulence" by Hamann (1980, 1981), and by Groenewegen, Lamers, and Pauldrach (1989). A physical interpretation of this microturbulence is offered by the work of Owocki, Castor, and Rybicki (1988), who found that their unstable time-dependent wind models are able to produce discrete absorption components that are stable over all phases of the chosen driving wave period of 4000 s. In the OCR model, the discrete components are due to the superposition of the absorption by density enhancements in the wind that are bounded on their inner edges by strong reverse shocks. Figure 12 of Owocki, Castor, and Rybicki reveals the highest velocity narrow absorption component predicted by their model to be at exactly the wind terminal velocity. The work of Prinja (1988) has shown that the time scale for evolution of discrete absorption components appears to be directly related to the stellar rotation period, with fast rotators like 68 Cyg and ξ Per showing much more rapid velocity evolution of the discrete absorption components than slow rotators like 19 Cep and HD 162978. Eventually, an outward-moving density enhancement will reach a velocity comparable to the terminal flow speed, and the absorption due to it will merge with that produced by other density enhancements farther out in the wind that are asymptotically approaching this velocity.

The narrow components are observed to evolve toward increasing velocity with time. We therefore conclude that $v_{NAC}(t \to \infty)$ provides a good indicator of v_∞; however, estimating this quantity observationally requires frequent (~hourly) *IUE* spectra taken over a sufficiently extensive period (~days), and such data are only available for a very few stars. It is therefore desirable to find a means to estimate v_∞ from a single "snapshot" UV spectrum. As shown by Howarth and Prinja (1989), this can be done; since the width of a discrete component decreases as its central velocity increases (i.e., as it evolves into a "narrow component"), an appropriate combination of the two should be approximately constant, and equal to $v_{NAC}(t \to \infty)$. From the time sequence data of Prinja, Howarth, and Henrichs (1987; ξ Per), Prinja and Howarth (1988; 68 Cyg), and Prinja (1988; 19 Cep, HD 162978), we confirm that the central velocity of the narrow absorption components, $\bar{v}_{NAC}$, plus the half-width at half-maximum depth of the model Doppler profiles fitted to them, $\overline{HWHM}_{NAC}$, is approximately constant and equal to $v_{NAC}(t \to \infty)$ during the time that the discrete absorption components are identifiable in isolated spectra, i.e., when they are present as narrow absorption features. (We define $\bar{v}_{\rm NAC}$ as the mean central velocity of the narrow components measured in all resonance line profiles in a given spectrum, taking into account only the most violet-shifted feature when multiple components are visible in a given line.)

To illustrate this, the central velocities of consecutive sequences of discrete absorption components in the spectra of 68 Cyg and 19 Cep are plotted in Figure 2 as a function of time (data from Prinja and Howarth 1988 and Prinja 1988). The sum $\bar{v}_{\rm NAC}$ + HWHM$_{\rm NAC}$ is also shown and is seen to be a good approximation to the velocity asymptotically approached by the narrow components. The time scale for the development and recurrence of the discrete features is a few days for the relatively rapid rotator 68 Cyg ($v_e \sin i = 315$ km s^{-1}; Uesugi and Fukuda 1982), whereas for the slow rotator 19 Cep ($v_e \sin i = 40$ km s^{-1}) it is much longer.

Also plotted in Figure 2 are the values of $v_{\rm black}$ derived from the saturated C IV profiles. It is clear that $v_{\rm black}$ can be identified with the asymptotic value of $\bar{v}_{\rm NAC}$ measured from long time sequences of data, at least for O stars. In fact, $v_{\rm black}$ is very stable, showing significantly less variation than the sum $v_{\rm NAC}$ + HWHM$_{\rm NAC}$, as well as being a more straightforward measurement to make. Hence it is potentially the most direct observational indicator of v_∞.

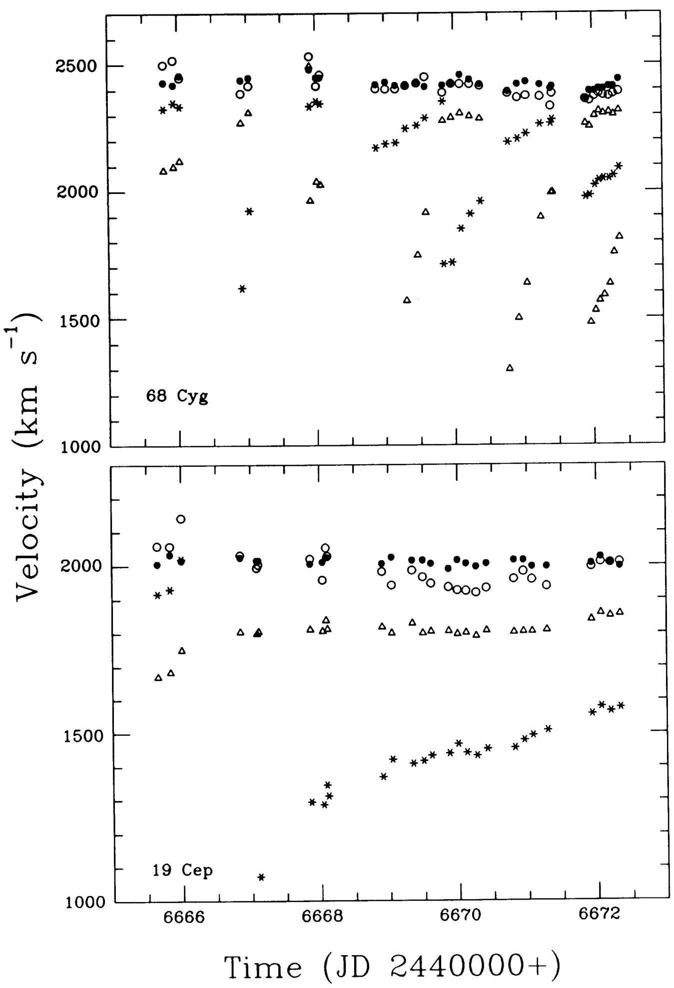

FIG. 2.—Central velocities of consecutive sequences of variable opacity enhancements in 68 Cyg (HD 203064) and 19 Cep (HD 209975) as a function of time. The sum $v_{\rm NAC}$ + HWHM$_{\rm NAC}$ (for the most blueshifted component) is also shown (*open circles*), together with the corresponding values of $v_{\rm black}$ derived from the C IV profiles (*filled circles*).

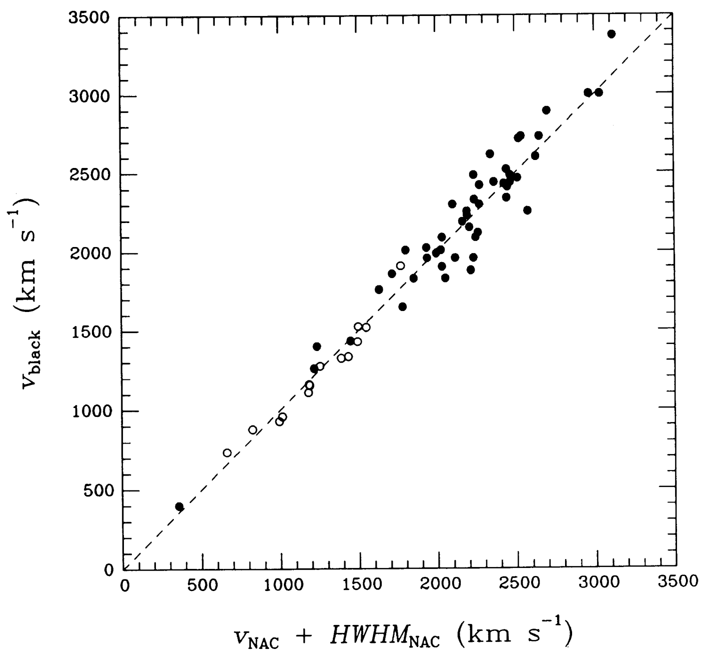

FIG. 3.—A comparison of $v_{\rm black}$, estimated from individual C IV profiles of O stars (*filled circles*) and B supergiants (*open circles*), and the corresponding sum of $\bar{v}_{\rm NAC}$ + HWHM$_{\rm NAC}$. The dashed line shows a one-to-one correspondence.

Among our total sample, 48 O stars and 13 B supergiants possess both saturated C IV profiles from which $v_{\rm black}$ can be measured *and* unsaturated Si IV profiles from which narrow component velocities and HWHMs can be measured. Figure 3 is a plot of $v_{\rm black}$ versus $\bar{v}_{\rm NAC}$ + HWHM$_{\rm NAC}$ for these stars (cf. Fig. 10 of Howarth and Prinja 1989). The dashed line corresponds to a 1:1 correlation, which the data fit very tightly (the product-moment correlation coefficient is $r = 0.98$).

The results presented here, and in Howarth and Prinja (1989), therefore show that, for OB stars, $v_{\rm black}$ and $\bar{v}_{\rm NAC}$ + HWHM$_{\rm NAC}$ measure the same quantity, which we have identified with v_∞. Since $v_{\rm black}$ is the simpler measurement and the more stable quantity, we preferentially adopt $v_\infty = v_{\rm black}$ for stars showing saturated P Cygni lines; C IV λ1550 nearly always provides the most easily measured profile. For stars without saturated profiles, but with readily identifiable narrow absorption components in an individual spectrum, we adopt $v_\infty = \bar{v}_{\rm NAC}$ + HWHM$_{\rm NAC}$.

The conclusion that, for saturated line profiles, the velocity range for black absorption extends as far as the wind terminal velocity but no further probably has a physical interpretation in that material moving at velocities in excess of the terminal flow speed is extremely rarefied (OCR). Interestingly, therefore, for saturated profiles the terminal velocity is given by the velocity where the black absorption starts to return to the continuum, just as in classical laminar flow Sobolev models.

III. RESULTS

a) O *Stars and* B *Supergiants*

Table 1 gives measurements of $v_{\rm max}$, $v_{\rm black}$, and $\bar{v}_{\rm NAC}$ for 181 O stars which have a saturated P Cygni profile and/or identi-

TABLE 1

STELLAR WIND VELOCITIES FOR O STARS

HD/BD/ CPD	Spectral Type	v_{max} (km s^{-1})	v_{black} (km s^{-1})	$\bar{v}_{NAC}$ (km s^{-1})	v_{∞} (km s^{-1})
108...........	O6: f?pe	2700	1960	1975	1960
1337..........	O9 III: (n)	2400	...	1840	1960
5005A........	O6.5 V ((f))	3350	...	2655	2835
12323........	ON9 V	1630	...	950	1105
12993........	O6.5 V	2750	...	2185	2290
13268........	O7	2370	...	1910	2070
13745........	O9.7 II ((n))	2400	1905	1920	1905
14434........	O5.5 V n((f))p	2300	1960	1805	1960
14633........	ON8 V	2100	...	1580	1690
14947........	O5 I f+	2550	1885	...	1885
15137........	O9.5 II–III (n)	2000	...	1530	1640
15558........	O5 III (f)	3200	2735	...	2735
15570........	O4 I f+	3200	2605	...	2605
15629........	O5 V ((f))	3200	2810	...	2810
15642........	O9.5 III: n	1800	1435	1230	1435
17505........	O6.5 V ((f))	2800	...	2160	2265
19820........	O8.5 III ((n))	2650	2255	2000	2255
24912........	O7.5 III (n)((f))	2500	2330	2130	2330
30614........	O9.5 Ia	1900	1590	...	1590
34656........	O7 II (f)	2500	2155	2020	2155
35619........	O7 V	2450	...	1775	1870
35921........	O9.5 III: n	2300	1990	1825	1990
36486........	O9.5 II	2300	...	1850	1995
36861........	O8 III ((f))	2650	...	2015	2125
36879........	O7 V (n)	2400	...	2110	2170
37022........	O6–O4 p var	1000	...	350	510
37043........	O9 III	2450	...	2070	2195
37742........	O9.7 Ib	2250	1860	1620	1860
39680........	O6 V: [n]pe var	1800	...	1540	1635
41161........	O8 V n	2400	...	1950	2035
42088........	O6.5 V	2215	...	2020	2155
46056........	O8 V n	1500	...	1200	1305
46150........	O5 V ((f))	3150	...	2780	2925
46223........	O4 V ((f))	3100	2910	...	2910
46485........	O7 V n(e)	2250	...	1730	1780
46966........	O8 V	2215	...	1945	2105
47129........	O8 p	2645	...	2255	2410
47432........	O9.7 Ib	2000	1590	...	1590
47839........	O7 V ((f))	2600	...	1925	2055
48099........	O7 V	3300	...	2840	2925
48279........	O8 V	1700	...	1515	1635
53975........	O7.5 V	2025	...	1705	1795
54662........	O6.5 V	2750	...	2265	2395
57060[a].......	O7 Ia: fp var	2135	1425	...	1425
57061........	O9 II	2350	1960	2000	1960
58509........	O8 V	1500	...	1165	1250
60369........	O9 III	2300	...	1725	1825
60848........	O8 V	1850	...	1620	1720
61347........	O9 I	2300	1775	...	1775
63005........	O6 V	2450	2120	2045	2120
66811........	O4 I (n)f	2700	2485	2215	2485
68450........	O9.7 Ib–II	2150	...	1905	1950
69464........	O6.5 Ib (f)	2600	2300	2035	2300
69648........	O8.5 I	2700	2090	2055	2090
73882........	O8.5 V ((n))	2550	...	2205	2315
74194........	O8.5 Ib (f)	2550	2160	...	2160
74920........	O8	2800	...	2365	2425
75222........	O9.7 Iab	2250	1840	...	1840
75759........	O9 V n	1400	...	1170	1245
76341........	O9 I	2250	...	1450	1500
76968........	O9.7 Ib	2400	1815	...	1815
90273........	O7	2500	...	2140	2240
91572........	O6 V ((f))	2650	2410	2245	2410
91651........	O9 V: n	1900	...	1600	1705
91824........	O7 V ((f))	2700	...	2240	2270
92554........	O9.5 II	1750	1260	1035	1260
92850........	O9.5 I	1900	...	1530	1615

TABLE 1—*Continued*

HD/BD/ CPD	Spectral Type	v_{max} (km s^{-1})	v_{black} (km s^{-1})	$\bar{v}_{NAC}$ (km s^{-1})	v_∞ (km s^{-1})
93129A	O3 I f	3950	3150	...	3150
93130	O6 III (f)	3100	2390	...	2390
93146	O6.5 V ((f))	2975	...	2400	2565
93204	O5 V ((f))	3250	2890	2530	2890
93205	O3 V	3630	3370	2845	3370
93206	O9.7 Ib: (n)	2350	1400	1020	1400
93222	O7 III ((f))	3050	...	2550	2645
93249	O9 III	2200	...	1685	1755
93250	O3 V ((f))	3350	...	3000	3160
93403	O5 III (f) var	2750	2615	2205	2615
93521	O9 V	1075	400	190	400
93843	O5 III (f) var	3150	2730	2405	2730
96715	O4 V ((f))	3430	3000	2845	3000
96917	O8.5 Ib (f)	2550	2000	...	2000
96946	O6 V:	2770	2465	2300	2465
99546	O8	2400	...	2070	2205
100213	O8.5 V n	1800	...	1530	1625
100444	O9 I	2600	...	2005	2090
101131	O6 V ((f))	3300	...	2535	2690
101190	O6 V ((f))	3100	...	2775	2945
101205	O7 III n((f))	3200	...	2500	2665
101298	O6 V ((f))	3300	2740	...	2740
101413	O8 V	2400	...	2095	2230
101436	O6.5 V	3100	2600	2490	2600
105056	ON9.7 Ia e	1325	680	...	680
105627	O9 II–III	2400	...	1830	1935
112244	O8.5 Iab (f)	2250	1575	...	1575
112784	O9.5 III	1650	...	1180	1275
113904	O9 II	2850	2255	2460	2255
115455	O7.5 III ((f))	2800	...	2100	2210
116852	O9 III	2600	2230	2035	2230
123008	ON9.7 Iab	2300	1250	...	1250
124314	O6 V (n)((f))	2700	...	2260	2425
124979	O8.5	3400	...	2685	2775
135240	O7.5 III ((f))	2700	...	2230	2390
135591	O7.5 III ((f))	2450	...	2055	2180
148937	O6.5 f?p	2650	...	2055	2215
149038	O9.7 Iab	2200	1830	1715	1830
149404	O9 Ia	2850	2450	...	2450
149757	O9 V	1640	...	1385	1470
150136	O5 III: n(f)	3700	3160	...	3160
151515	O7 II (f)	2800	2520	2230	2520
151804	O8 Ia f	2250	1445	...	1445
152218	O9.5 IV (n)	2125	...	1925	2020
162233	O6 III: (f)p	3200	2730	2345	2730
152246	O9 III–IV ((n))	2200	...	1610	1670
152247	O9.5 II–III	2800	...	2100	2235
152248	O7 Ib: (n)(f)p	2700	2420	2040	2420
152249	OC9.5 Iab	2350	2010	1610	2010
152405	O9.7 Ib–II	2200	...	1750	1825
152408	O8: Ia fpe	2200	955	...	955
152424	OC9.7 Ia	2175	1760	1495	1760
152590	O7.5 V	2150	...	1650	1745
152623	O7 V (n)((f))	3300	...	2830	3015
152723	O6.5 III (f)	3500	3000	2835	3000
153426	O9 II–III	2350	...	2065	2160
153919	O6.5 Ia f+	2650	1820	...	1820
154368	O9.5 Iab	2200	1850	...	1850
155806	O7.5 V [n]e	2900	...	2230	2390
156292	O9.5 III	1530	...	1235	1320
156359	O9 III	2175	...	1800	1885
157857	O6.5 III (f)	3050	2300	2150	2300
159176	O7 V + O7 V	3000	...	2475	2555
162978	O7.5 II ((f))	2800	2350	...	2350
163758	O6.5 Ia f	2675	2420	...	2420
163892	O9 IV ((n))	1575	...	1285	1370
164492	O7.5 III ((f))	1700	...	1495	1580
164794	O4 V ((f))	3550	2750	...	2750

TABLE 1—*Continued*

HD/BD/ CPD	Spectral Type	v_{max} (km s^{-1})	v_{black} (km s^{-1})	$\bar{v}_{NAC}$ (km s^{-1})	v_{∞} (km s^{-1})
165052.......	O6.5 V (n)((f))	2800	...	2205	2295
167263.......	O9.5 II–III ((n))	2450	...	2025	2155
167264.......	O9.7 Iab	2100	...	1735	1795
167659.......	O7 II (f)	2730	2440	2135	2440
167771.......	O7 III: (n)((f))	2700	2485	2320	2485
167971.......	O8 Ib (f)p	2275	2185	...	2185
168075.......	O6 V ((f))	3200	2845	...	2845
168076.......	O4 V ((f))	3550	3305	...	3305
168941.......	O9.5 II–III	2250	...	1665	1755
171589.......	O7 II (f)	3200	2935	...	2935
175754.......	O8 II ((f))	2700	2060	...	2060
175876.......	O6.5 III (n)(f)	2900	2430	2260	2430
186980.......	O7.5 III ((f))	2550	...	2070	2205
188001.......	O7.5 Ia f	2330	1980	...	1980
188209.......	O9.5 Iab	2100	1650	1470	1650
190429A	O4 I f+	2850	1880	2020	1880
190864.......	O6.5 III (f)	2800	2440	2250	2440
191423.......	O9 III: n	1350	...	750	800
192639.......	O7 Ib (f)	2700	2180	...	2180
193322.......	O9 V: ((n))	1800	...	1510	1605
193443.......	O9 III	2500	...	2090	2250
193514.......	O7 Ib (f)	2750	2190	2055	2190
199579.......	O6 V ((f))	3300	2715	2275	2715
201345.......	ON9 V	1550	...	1280	1380
202124.......	O9.5 Iab	2100	1820	...	1820
203064.......	O7.5 III: n((f))	2800	2340	2310	2340
206267.......	O6.5 V ((f))	3225	...	2535	2680
207198.......	O9 Ib–II	2450	2090	1905	2090
209481.......	O9 V:	2250	...	1815	1925
209975.......	O9.5 Ib	2400	2010	1835	2010
210809.......	O9 Iab	2750	2135	...	2135
210839.......	O6 I (n)fp	2600	2300	...	2300
214680.......	O9 V	1375	...	1075	1120
215835.......	O6 V (n)	3275	2810	...	2810
217086.......	O7 V n	3000	2510	...	2510
218195.......	O9 III	2300	...	1895	1985
218915.......	O9.5 Iab	2425	1830	1895	1830
235673.......	O6.5 V	2800	2485	...	2485
242908.......	O4 V (n)	3200	...	2645	2785
303308.......	O3 V ((f))	3300	3035	...	3035
+34°1058 ...	O8	2315	2025	1860	2025
+60°594.....	O9 V	1550	...	1350	1435
+60°2522 ...	O6.5 (n)(f)p	2600	2035	...	2035
−59°2600 ...	O6 V ((f))	3400	...	2940	3065
−59°2603 ...	O7 V ((f))	2050	...	1695	1795
−59°2641 ...	O5 V	3200	2870	...	2870

[a] See text, § III*a*, for a discussion of the data sources for this star.

fiable narrow components. With only one exception,[2] these data are reproduced from Howarth and Prinja (1989, where they are respectively denoted as v_*, v_b, and v_c), who give details of data reduction techniques and procedures used for modeling the discrete absorption components, as well as primary sources for the adopted spectral types. The final column of Table 1 lists the adopted values of v_{∞}, which correspond to v_{black} for stars having saturated lines (C IV in all cases except the five ON stars, for which N V was used), and to $\bar{v}_{NAC} + \text{HWHM}_{NAC}$, otherwise. The velocities have measurement errors estimated to be $\lesssim 100$ km s^{-1}.

Corresponding results for 70 B supergiant stars having spectral types of B3 or earlier are listed in Table 2. Spectral types were again taken from the primary sources listed by Howarth and Prinja (1989), supplemented where necessary by classifications from Hiltner (1956), Lesh (1968), and Morgan, Code, and Whitford (1956). We restrict ourselves to B0–B3 supergiants in the knowledge that the C IV resonance line still provides a sensitive diagnostic of mass loss for these stars (e.g., Heck *et al.* 1984; Walborn and Nichols-Bohlin 1987). As for the bulk of the O stars, the values of v_{edge} and v_{black} listed in

[2] The exception is HD 57060 (=UW CMa), for which the value of v_{black} ($=v_{\infty}$) listed in Table 1 is 400 km s^{-1} larger than that listed by Howarth and Prinja (1989). Significant variations in the C IV profile of this system occur during its 4.39 day orbital cycle (Heap 1982). The terminal velocity of 1425 km s^{-1} listed in Table 1 was measured from SWP 3390, which corresponds to phase 0.573 (Stickland 1989), with the O7 Ia:fp primary in front. On SWP 9620 (phase 0.071; secondary in front) v_{black} = 1025 km s^{-1} was measured from the C IV profile; we consider that this value is likely to reflect the terminal velocity of the secondary star, for which a spectral type of O9.5 V–B0 V has been inferred indirectly (van Genderen *et al.* 1988). We also note that some of the terminal velocities derived for other spectroscopic binaries in our sample could be affected by orbital motions of up to ~200 km s^{-1}.

TABLE 2

STELLAR WIND VELOCITIES FOR B SUPERGIANTS

HD	SWP	Spectral Type	v_{esc} [a] (km s^{-1})	v_{edge} (km s^{-1})	v_{black} (km s^{-1})	$\bar{v}_{NAC}$ (km s^{-1})	v_∞ (km s^{-1})
2905	14902	BC0.7 Ia	557	1345	1105	...	1105
5045	9334	B3 Ia	(400)	565	405	...	405
13854	2737	B1 Ia	(513)	1105	920	...	920
14143	9435	B2 Ia	376	1005	645	...	645
14818	9416	B2 Ia	407	820	565	...	565
24398	6454	B1 Ib	522	1335	...	1215	1270
29138	10051	B1 Iab	(531)	1300	...	1140	1315
37128	(PH86)[b]	B0 Ia	700	1980	1910	1725	1910
38771	(PH86)[b]	B0.5 Ia	580	1800	1525	1425	1525
40111	18943	B1 Ia	663	1560	...	1340	1465
41117	4374	B2 Ia	399	850	510	...	510
43384	4656	B3 Iab	442	715	...	600	710
47420	9895	B1 Ib	(558)	1250	960	885	960
52382	27404	B1 Ib	(558)	1245	900	...	900
53138	13564	B3 Ia	431	845	...	750	830
58510	21677	B1 Iab	(531)	1375	930	910	930
77581	22301	B0.5 Iae	(590)	1310	1105	...	1105
86606	14677	B1 Ib	(558)	615	...	420	490
91316	(PH86)[b]	B1 Iab	(531)	1350	1110	1090	1110
91452	20622	B0 Ia	(713)	2095	1635	...	1635
91943	23760	B0.5 Ib	(558)	1690	...	1255	1405
91969	9076	B0 Ia	(713)	1785	1545	...	1545
92964	6316	B2.5 Ia	(410)	880	435	...	435
93840	21525	B2 Ib	(416)	1255	...	995	1160
94493	21505	B0 Iab	(702)	1545	...	1345	1495
94909	14810	B0 Ia	(713)	1250	1050	...	1050
96248	7702	BC1.5 Iab	(440)	880	675	...	675
97522	31295	B1.5 Ib	(436)	1300	...	1040	1190
97707	31272	B2 Ib	(416)	1050	870	...	870
99857	22170	B0.5 Ib	(558)	1720	...	1600	1705
99953	9074	B1.5 Ia	(444)	805	510	...	510
100276	22147	B1 Ib	(558)	1830	1430	1390	1430
104683	22169	B1 Ib	(558)	1345	...	1020	1145
106343	6320	B1.5 Ia	(444)	1275	795	...	795
109399	20308	B0.5 Ib	(558)	1565	1325	1280	1325
109867	14928	B0.7 Ib	(558)	1635	1155	1085	1155
113012	22168	B0.2 Ib	(625)	1445	...	1075	1215
115842	27405	B0.5 Ia	(590)	1530	1180	...	1180
116084	6322	B2.5 Ib	(467)	1040	550	...	550
119608	5647	B1 Ib	(558)	1120	880	705	880
148379	4349	B1.5 Iap	(444)	685	510	...	510
148422	23529	B0.5 Ia	(590)	2185	1335	1245	1335
148688	1871	B1 Ia	(513)	870	725	...	725
150898	9267	B0.5 Ia	(590)	1310	...	1200	1300
152235	16205	B0.5 Ia	(590)	1445	850	...	850
152236	8831	B1.5 Ia$^+$	441	675	390	...	390
152667	(H84b)[c]	B0 Ia((n))	(590)	1565	795	...	795
154090	14828	B1 Ia	554	1305	915	...	915
155985	7742	B0.5 Ia	(590)	1280	...	1190	1225
157038	30759	B3 Iap	(442)	1015	525	...	525
157246	(PH86)[b]	B1 Ib	(558)	1000	735	505	735
160993	23541	B1 Ia	(513)	1375	...	1200	1320
163181	2235	BN0.5 Iap	(590)	885	520	...	520
163522	32073	B1 Iap	(513)	1490	1240	...	1240
164402	18147	B0 Ib	658	2115	...	1585	1650
165024	6331	B2 Ib	(416)	1130	...	1000	1130
167264	6490	B0 Ia	732	2020	1640	...	1640
167402	23528	B0 Ib	(691)	2185	...	1905	2005
167756	30453	B0.5 Ia	(590)	2285	...	1700	1865
178487	26986	B0 Ia	(713)	1660	...	1430	1520
179407	23833	B0.5 Ib	(558)	1670	...	1470	1585
185859	14207	B0.5 Ia	(590)	2135	...	1455	1715
190066	18310	B1 Iab	(531)	1570	1275	1155	1275
190603	14942	B1.5 Ia$^+$	452	670	485	...	485
191877	14825	B1 Ib	(558)	1310	1160	1020	1160
198478	13907	B3 Ia	393	655	470	...	470
204172	6481	B0 Ib	644	2015	...	1500	1630
206165	6336	B2 Ib	416	910	640	...	640
213087	2736	B0.5 Ib	552	1595	1520	1470	1520
235783	21706	B1 Ib	(558)	1305	1070	...	1070

[a] Values in parentheses are means for the spectral type.
[b] Data from Prinja and Howarth 1986.
[c] Measurements from the mean spectrum constructed by Howarth 1984*b*.

Table 2 were determined from the C IV profiles, while the values of $\bar{v}_{\rm NAC}$ represent the mean values found from unsaturated C IV, Si IV and N V resonance line profiles. Narrow components may be present in other lines (e.g., HD 152667 shows such features in C II λ1335 and Fe III λ1900; Howarth 1984*a*, *b*), but we have not carried out a systematic study of their occurrence.

The sample represents all of the B0–B3 supergiants which had high-resolution *IUE* spectra available from the Rutherford Appleton Laboratory World Data Centre archive at the time of our investigation (mid-1989). Prinja (1989) examined the UV spectra of normal nonsupergiant B0–B5 stars and found no evidence of narrow absorption components or of saturated stellar wind profiles; the wind terminal velocities of these stars cannot, therefore, be safely determined from direct measurement of *IUE* data.

Table 3 lists the mean terminal velocities found for each spectral type in luminosity classes I, III, and V in our sample. (We ignored "f" qualifiers and omitted the extreme BI$^+$ supergiants and the OBNC stars from these means, together with HD 93521, which has very peculiar profiles—see Prinja and Howarth 1986.) Table 3 shows that, for spectral types running from O4 to O9.5, the mean terminal velocities decline quite steeply for the dwarfs and giants, falling from 3000 km s^{-1} to 1400 km s^{-1} and from 2800 km s^{-1} to 1500 km s^{-1}, respectively, while for the supergiants the decline is much less steep (from 2300 km s^{-1} to 1800 km s^{-1}). The mean terminal velocities of the B supergiants continue this decline, falling from 1600 km s^{-1} at B0 to 600 km s^{-1} at B3.

b) Wolf-Rayet Stars

Figure 1 shows the C IV profile observed in the spectrum of the WC5 star HD 165763. The velocity corresponding to the black absorption edge, $v_{\rm black}$, is marked, as is our estimate for the position of $v_{\rm edge}$. Determining the position of $v_{\rm edge}$ is often difficult in O star spectra because of the need to estimate where unit continuum lies; in WR spectra, with their many blended emission lines, it can be even more of a problem. By contrast, the determination of $v_{\rm black}$ is straightforward, as Figure 1 shows. We assume that, as for the O stars, it provides a reliable measurement of v_∞; this assumption is justified by the comparisons with other indicators of v_∞ discussed in § III*c*.

Thirty-five Galactic Wolf-Rayet stars had well-exposed high-resolution *IUE* spectra available in the Rutherford Appleton Laboratory World Data Centre archive at the time of our investigation. The velocity measurements made from these spectra are presented in Table 4. For the single WN stars in our sample, the N V resonance line always exhibits a saturated absorption profile, as does the C IV resonance doublet for all but the WN3 star; Si IV shows saturated absorption for the WN6–WN8 types. The subordinate lines He II λ1640 and N IV λ1718 almost never reach zero intensity.

For the single WC stars, the C IV and Si IV resonance lines always have saturated absorption, as do the C II resonance line profiles for all but the WC5 types. The absorption profiles of the C III λ1175 and λ1247 subordinate lines always reach zero intensity in the spectra of the single WC stars, whereas the absorption profile of C III] λ1909 never does.

We have measured the value of $v_{\rm black}$ for all saturated absorption profiles mentioned above (these measurements are given in roman type in Table 4). For unsaturated absorption profiles (including, in the case of WR binaries, profiles which do not reach zero intensity because of the presence of a residual O star continuum), we have measured the velocity at the deepest point in the absorption profile (given in italics in Table 4). If a flat-bottomed but unsaturated profile is present, we measured the blueward edge of the flat region. These velocities are parenthesized in Table 4.

Figures 4*a*, 4*b*, and 4*d* show examples of the velocities measured in the profiles of C III λ1247, C II λ1335, and C III] λ1909

TABLE 3

MEAN AND RANGE OF OB STAR TERMINAL VELOCITIES AS A FUNCTION OF SPECTRAL TYPE AND LUMINOSITY CLASS

	I			III			V		
Spectral Type	$\bar{v}_\infty$ (km s^{-1})	Range (km s^{-1})	N[a]	$\bar{v}_\infty$ (km s^{-1})	Range (km s^{-1})	N[a]	$\bar{v}_\infty$ (km s^{-1})	Range (km s^{-1})	N[a]
O3	3150	...	1	...	...	...	3190	3035–3370	3
O4	2325	1880–2605	3	...	...	...	2950	2750–3305	5
O5	1885	...	1	2810	2615–3160	4	2875	2810–2925	4
O5.5	...	...	...	...	...	...	1960	...	1
O6	2300	...	1	2560	2390–2730	2	2570	1635–3065	12
O6.5	2180	1820–2420	3	2545	2300–3000	4	2455	2155–2835	10
O7	2055	1425–2420	4	2600	2485–2665	3	2295	1780–3015	10
O7.5	1980	...	1	2175	1580–2390	7	1975	1745–2390	3
O8	1530	955–2185	3	2125	...	1	1755	1250–2230	7
O8.5	1955	1575–2160	4	2255	...	1	1970	1625–2315	2
O9	1990	1500–2450	5	1875	800–2250	9	1500	1120–1925	7
O9.5	1765	1590–2010	7	1505	1275–1990	4	...	...	...
O9.7	1735	1400–1860	7	...	...	...	...	...	...
B0	1535	795–2005	11	...	...	...	...	...	...
B0.2	1215	...	1	...	...	...	...	...	...
B0.5	1405	850–1865	14	...	...	...	...	...	...
B0.7	1155	...	1	...	...	...	...	...	...
B1	1065	490–1465	20	...	...	...	...	...	...
B1.5	750	510–1190	4	...	...	...	...	...	...
B2	790	510–1160	7	...	...	...	.	...	...
B2.5	490	435–550	2	...	...	...	...	...	...
B3	590	405–830	5	...	...	...	...	...	...

[a] Number of stars.

1990ApJ...361..607P

TABLE 4

MAXIMUM VELOCITIES AT WHICH THE ABSORPTION MINIMUM OCCURS IN THE STRONGEST STELLER WIND LINES OF WN AND WC STARS

HD	Spectral Type	SWP	C III λ1175.7	N V λ1238.8	C III λ1247.4	C II λ1334.5	Si IV λ1393.8	Si IV λ1402.8	C IV λ1548.2	He II λ1640.4	N IV λ1718.6	C III λ1908.7	Mean[a] (excluding C IV)
104994	WN3	7020	...	3120	...	...	...	...	...	...	...	...	...
187282	WN4	15101	...	2290	...	...	...	...	2270	*1785*	(1750)	...	1940
65865	WN4.5	29703	...	...	...	...	...	...	1475	1345	1400	...	1375
190918	WN4.5 + O9.5 Ib	14715	...	1565	...	...	(1510)	(1425)	1625	...	*1560*	...	1515
50896	WN5	(HP)[b]	...	1725	...	...	(1635)	(1580)	1720	*1780*	(1620)	...	1670
193077	WN5 + abs	15641	...	(1230)	...	...	*1230*	*1195*	1345	*1250*	*1200*	...	1220
193576	WN + O6	26007	...	1250	...	...	...	...	1785	(1770)	(1400)	...	1475
143414	WN6	16976	...	1575	...	...	1600	1590	1590	*1325*	*1320*	...	1480
191765	WN6	4088	...	1910	...	...	*1795*	*1770*	1905	(1795)	(1705)	...	1795
192163	WN6	30793	...	(1380)	...	...	1570	1565	1605	(1610)	(1610)	...	1545
211853	WN6 + O	14143	...	1150	...	...	(1465)	(1485)	1785	...	*1700*	...	1450
62910	WN6-C4	27473	...	...	...	...	1530	1555	1600	(1335)	*1600*	...	1505
151932	WN7	4334	...	1550	...	...	1400	1380	1365	(1175)	*1160*	...	1335
92740	WN7 + abs	27342	...	...	...	...	1770	1770	1790	*1050*	(1440)	...	1510
93131	WN7 + abs	27341	...	(2325)	...	...	2130	2040	2155	*1785*	*1635*	...	1985
93162	WN7 + abs	15025	...	...	...	...	*2105*	*2010*	2455	*1770*	*1575*	...	1865
214419	WN + O	13996	...	...	...	...	1680	1440	1690	(1325)	*910*	...	1340
86161	WN8	13893	...	(770)	...	...	755	755	(855)	*655*	*660*	...	720
96548	WN8	6927	...	955	...	...	955	920	(975)	(920)	*890*	...	930
115473	WC5	15105	...	...	2440	...	3025	2830	3225	...	...	...	2765
165763	WC5	2872	...	...	(2495)	*2200*	2400	2405	2415	...	...	*2160*	2330
76536	WC6	10113	...	...	(2450)	(2025)	2080	2070	2055	...	...	*1840*	2095
92809	WC6	15558	...	...	2380	(2150)	2220	2250	2280	...	...	*2200*	2240
119078	WC7	20280	1715	...	(1845)	1820	1850	1785	1770	...	...	*1485*	1750
156385	WC7	15130	...	...	2255	(2040)	2185	2100	2045	...	...	*1930*	2100
97152	WC7 + O5–7	15107	1625	...	1910	*1555*	1750	1670	1645	...	...	*1505*	1670
152270	WC7 + O5–8	15129	2185	...	(2130)	(2150)	2300	2310	2270	...	...	*2050*	2190
192641	WC7 + O5	31507	...	...	*1760*	*1680*	1820	1920	1885	...	...	*1955*	1830
193793	WC7 + O4–5	31504	...	...	(2600)	*1510*	*2635*	*2645*	2900	...	...	*2760*	2430
192103	WC8	22861	1505	...	1300	(1495)	1480	1460	1405	...	...	*1280*	1420
68273	WC8 + O9 I	3377	1520	...	(1040)	*1045*	1415	1405	1415	...	...	*1165*	1265
168206	WC8 + O8–O9 IV	34037	...	...	...	1715	1820	1885	1890	...	...	*1450*	1720
136488	WC9	13816	...	...	...	1275	1140	(1120)	1160	...	...	(1105)	1160
157451	WC9	16835	...	...	...	1300	1125	1095	1070	...	...	*990*	1130
164270	WC9	8156	...	...	1130	1190	1140	1025	1090	...	...	*820*	1060

NOTE.—Measurements of v_{black} are indicated by values in roman type, the velocities of the deepest points in unsaturated absorption profiles are in italics, and the blueward edge of flat regions in unsaturated profiles are enclosed in parentheses.

[a] " Mean " values in this column exclude the C IV values, to facilitate comparison between the two measures.

[b] Values measured using the mean spectrum constructed by Howarth and Phillips 1986.

in the spectrum of the WC8 + O9 I binary γ Velorum. This spectrum (SWP 3377), obtained and first illustrated by Kondo, Feibelman, and West (1982), was taken at phase 0.534 (WC8 star in front), so that the orbital radial velocities of the component stars are minimized. The C IV λ1550 profile (Fig. 4*c*) shows evidence of the winds from both components. We identify the black absorption edge velocity of -1415 km s^{-1} (*short vertical arrow*) with the wind of the WC8 component; this value is close to the velocities measured for the C III lines (Table 4), which can arise from only the WC8 wind. It agrees well with the terminal velocity of 1520 ± 200 km s^{-1} determined by Barlow, Roche, and Aitken (1988) for γ Vel from the profile of the 12.8 μm [Ne II] emission line, which is formed far out in the wind. The velocity of 2370 km s^{-1} which we identify with v_{black} for the O9 I component is indicated by the long vertical arrow in Figure 4*c*; it does not reach zero intensity because the O star wind does not absorb the WC8 continuum in the composite spectrum (the composite C IV profile is black as far as -1415 km s^{-1} because the absorption profiles of both stars are black as far as this velocity). With this interpretation, the C IV profile shown in Figure 4*c* implies that at 1540 Å the O9 I star continuum is 0.7 ± 0.2 mag brighter than that of the WC8 star. The implied terminal velocity of the O star falls within the range found for single O9 supergiants (Table 3).

Other WR binaries where we see evidence for a composite C IV profile are the WC7 binaries HD 87152, HD 152270, and HD 192641, for which we estimate O star wind terminal velocities of 2460, 2900, and 2750 km s^{-1}, respectively.

The *IUE* spectrum (SWP 26007) chosen for V444 Cyg (=HD 193576) came from the study of Shore and Brown (1988) and corresponds to phase 0.997 (WN5 star in front) so that, as with γ Vel, orbital motions relative to the observer are minimized. The *IUE* SWP images chosen for the spectroscopic binaries HD 190918 and HD 211853 were taken at phases 0.93 and 0.98, respectively.

Table 5 lists the values of v_{edge} and v_{black} ($=v_\infty$) that were measured for each of the Wolf-Rayet stars from their saturated C IV absorption profiles, except (*a*) for the case of the WN3 star HD 104994, where C IV λ1550 is undetectable and we instead used N V λ1240, and (*b*) for the case of the three WC9 stars, for which we adopted the velocities measured from C II λ1335, since C^+ is the dominant ion in the spectra of these stars.

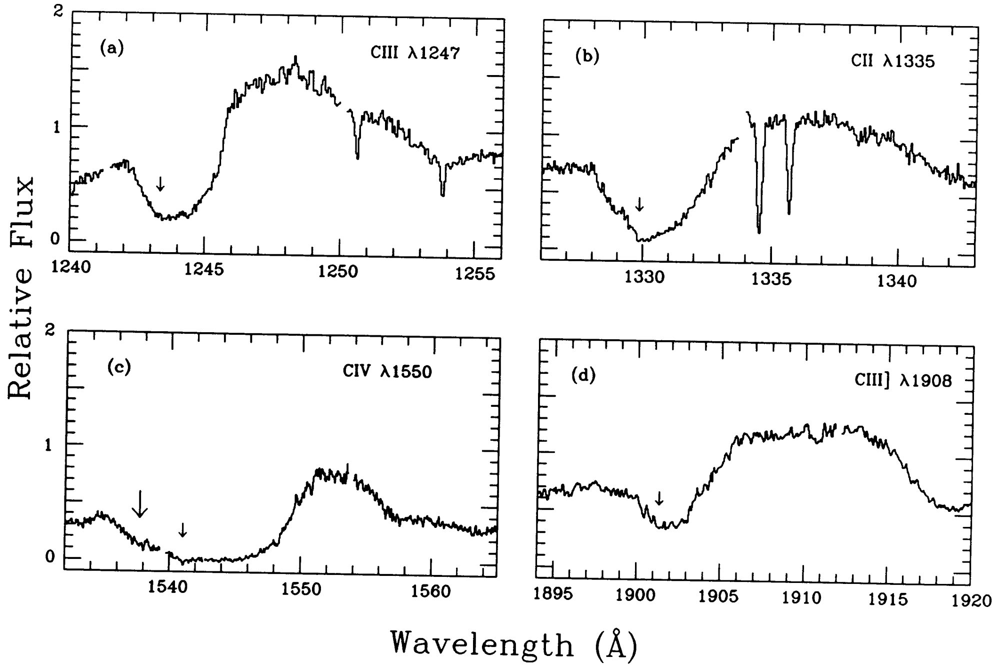

FIG. 4.—Examples of carbon line stellar wind profiles for HD 68273 (γ Vel; WC8 + O9 I). The maximum wind velocities at which the absorption minimum occurs in the WR wind (*short arrow*) and O star wind (*long arrow*) are indicated.

TABLE 5

STELLAR WIND VELOCITIES AND MASS-LOSS RATES FOR WR STARS

HD	WR[a]	SWP	Spectral Type	v_{edge} (km s^{-1})	v_∞ (km s^{-1})	log($\dot{M}$) ($M_\odot$ yr^{-1})
104994.......	46	7020	WN3	3235	3120	...
187282.......	128	15101	WN4	2515	2270	...
65865........	10	29703	WN4.5	2035	1475	...
190918.......	133	14715	WN4.5 + O9.5 Ib	1770	1625	−4.52
50896........	6	(HP)	WN5	3140	1720	−4.12
193077.......	138	15641	WN5 + abs	1650	1345	−4.73
193576.......	139	26007	WN5 + O6	2325	1785	−4.62
143414.......	71	16976	WN6	2880	1590	...
191765.......	134	4088	WN6	2775	1905	−4.13
192163.......	136	30793	WN6	2700	1605	−4.02
211853.......	153	14143	WN6 + O	1900	1785	...
62910........	8	27473	WN-C4	2540	1600	...
151932.......	78	4334	WN7	2125	1365	−4.31
92740........	22	27342	WN7 + abs	2550	1790	...
93131........	24	27341	WN + abs	2700	2155	...
93162........	25	15025	WN7 + abs	3130	2455	...
214419.......	155	13996	WN7 + O	1920	1690	< −4.61
86161........	16	13893	WN8	1000	855	...
96548........	40	6927	WN8	1215	975	...
115473.......	52	15105	WC5	4250	3225	...
165763.......	111	2872	WC5	3500	2415	−4.50
76536........	14	10113	WC6	2850	2055	...
92809........	23	15558	WC6	3400	2280	...
119078.......	57	20280	WC7	2300	1770	...
156385.......	90	15130	WC7	2450	2045	< −4.46
97152........	42	15107	WC7 + O5–7	2850	1645	...
152270.......	79	15129	WC7 + O5–8	3300	2270	−3.98
192641.......	137	31507	WC7 + O5	2550	1885	−4.48
193793.......	140	31504	WC7 + O4–5	3200	2900	−4.10
192103.......	135	22861	WC8	1920	1405	−4.36
68273........	11	3377	WC8 + O9 I	1680	1415	−4.09
168206.......	113	34037	WC8 + O8–O9 IV	2025	1890	≤ −4.38
136488.......	69	13816	WC9	1615	1275	...
157451.......	92	16835	WC9	1870	1300	...
164270.......	103	8156	WC9	1310	1190	≤ −4.54

[a] Numbers from the catalog of van der Hucht *et al.* 1981.

The final column in Table 4 lists the mean of the absorption velocities, excluding C IV, measured for each WR star. Comparison of these mean velocities with the C IV velocities (which we generally adopt as v_∞) shows agreement to within 120 km s^{-1} for 13 out of 16 WC stars and for 10 out of 19 WN stars. When present, the velocities given by the N V and Si IV resonance lines show good agreement with the C IV velocities. In the case of the WC stars, the C III $\lambda1175$ and $\lambda1247$ excited state line velocities and the C II resonance line velocities are in general agreement with the C IV velocities.

Hillier (1989) has suggested that the line-center optical depth of C IV $\lambda1550$ can be so large ($\sim 10^9$) in the winds of WC stars that broad Lorentzian wings will affect its profile. However, we interpret the fact that the C IV black absorption edge velocities measured by us for the WC stars agree so well with the velocities measured from the Si IV, C II, and C III lines (Table 4) as indicating that Lorentzian damping wings do not significantly affect the position of the C IV black absorption edge in the spectra of these stars (or that all these lines have similar optical depths, which seems unlikely).

Single Wolf-Rayet stars are, in general, not observed to exhibit NACs in their UV P Cygni profiles (e.g., St-Louis, Willis, and Smith 1988), presumably because the UV resonance line absorption profiles in their spectra are almost always saturated. Some WR stars in spectroscopic binary systems have, however, been observed to exhibit NACs in their UV resonance line profiles. This phenomenon could be due to absorption of the companion O star continuum by the WR wind at large radii. Fitzpatrick, Savage, and Sitko (1982) observed an NAC in the Si IV profile of the WR binary HD 193793, with a central velocity of 2700 km s^{-1} and a HWHM of 125 km s^{-1}, which was stable in velocity and strength over a period of 5 months. The terminal wind velocity of 2825 km s^{-1} given by these data is consistent with the value of 2900 km s^{-1} implied for the WC7 star by the C IV black absorption edge (Table 5). In the C IV and Si IV profiles of the WR binary HD 193077, Koenigsberger and Auer (1987) found absorption features at -1250 km s^{-1}, with widths of $\sim$200 km s^{-1}. The implied terminal velocity of $\sim$1350 km s^{-1} is again consistent with the value of 1345 km s^{-1} listed in Table 5.

c) *Comparison with Other Estimates of v_∞*

Groenewegen, Lamers, and Pauldrach (1989) have recently derived terminal velocities for the winds of 26 O stars, plus the B0 supergiant ϵ Ori, from *IUE* observations of resonance line profiles. They used a profile-fitting method which incorporates a turbulence parameter and therefore also derived terminal velocities significantly lower than v_{max}. Their values show good agreement with those derived here (Table 1): the mean ratio (ours/theirs) is 0.97 ± 0.11.

For the 10 WR stars in common, our values of v_{edge} (Table 5) show agreement with those measured by Willis (1982; his "v_a"). On the other hand, there is no simple correspondence between his "centre of the violet-displaced absorption component," v_0, and the absorption velocities listed in Table 4.

Hillier (1987*b*) deduced a maximum flow velocity of 1600–1700 km s^{-1} in the line formation region of the WN5 star HD 50896 from detailed modeling of the UV, optical, and IR line profiles, and he was forced to invoke a further acceleration of the wind at much larger radii in order to explain the much higher UV violet absorption edge velocities. (Hamann, Schmutz, and Wessolowski 1988 also reached this conclusion.) However, the terminal velocity of 1720 km s^{-1} given by the black absorption edge of C IV in the mean spectrum of Howarth and Phillips (1986; our Table 5) effectively eliminates the need to invoke further wind acceleration at large radii.

Torres, Conti, and Massey (1986) estimated wind terminal velocities for a large sample of WC stars by fitting the profiles of optical emission lines and extrapolating a line width versus excitation potential (EP) diagram to zero EP. For the 13 stars in common we find that their method gives velocities that are larger than the terminal velocities listed in Table 5 by an average factor of 1.21 ± 0.17.

Williams and Eenens (1989) have recently measured the velocities of the He I 2.058 μm violet-displaced absorption line in the spectra of eight Wolf-Rayet stars and have argued that the absorption occurs far out in the winds, so that the velocities are representative of the wind terminal velocities. Of the five stars in common with our data, four give agreement to better than 80 km s^{-1} between the values of v_∞ listed in Table 5 and the values of v_e (the central absorption velocity v_0 + HWHM) that they measured from the He I 2.058 μm absorption profiles. The fifth object is the WN7 + O system HD 214419, for which our value of $v_\infty = 1690$ km s^{-1} exceeds by 700 km s^{-1} that for v_e measured by Williams and Eenens.

Schmutz, Hamann, and Wessolowski (1989) have estimated wind terminal velocities for 30 WR stars from profile fits to (or, in some cases, from the observed maximum line widths of) He I and He II emission-line profiles in the 0.5–1.1 μm spectral region. There are 20 stars in common with our WR sample. For the five WC stars in common, the velocities derived by Schmutz *et al.* are a factor of 1.22 ± 0.11 larger than those given by the C IV $\lambda1550$ black absorption edge (as discussed earlier, the velocities obtained from the Si IV, C II, and C III UV absorption profiles in WC star spectra are in agreement with those derived from C IV; Table 4). The eight WN4.5, WN5, WN6, and WN8 stars in common show good agreement between the terminal velocities derived by Schmutz *et al.* from the 0.6–1.1 μm line widths and the terminal velocities derived here (the mean ratio is 1.00 ± 0.08). However, the velocities derived by Schmutz *et al.* for the four WN7 stars in their sample, and for the WN3 and WN4 stars HD 104994 and HD 187282, are much smaller than the terminal velocities derived here (the mean ratio is 0.65 ± 0.14). These stars have the weakest emission lines in their WR sample, and we interpret the above discrepancy as implying that the 0.6–1.1 μm helium emission line width fits of Schmutz *et al.* do not yield the terminal velocity in the case of these weak-lined WR stars. This conclusion also appears to apply to the 2.058 μm He I absorption profile measured by Williams and Eenens (1989) in the spectrum of the WN7 system HD 214419 (see above).

IV. DISCUSSION

Figure 5 shows a plot of v_{edge} versus v_∞ for the O stars, B supergiants, and WR stars in our sample. For given values of v_∞, the WR stars can be seen to have systematically higher values of v_{edge}. The WR stars have significantly ($\sim 10\times$) higher rates of mass loss, $\dot{M}$, suggesting the possibility of a causal relationship, which we now investigate.

The last column of Table 5 lists mass-loss rates for those Wolf-Rayet stars in our sample which have been observed at radio wavelengths. Since the major WR radio survey by Abbott *et al.* (1986), a number of effects have been noted which lead to changes in their derived mass-loss rates.

1. Van der Hucht, Cassinelli, and Williams (1986) showed

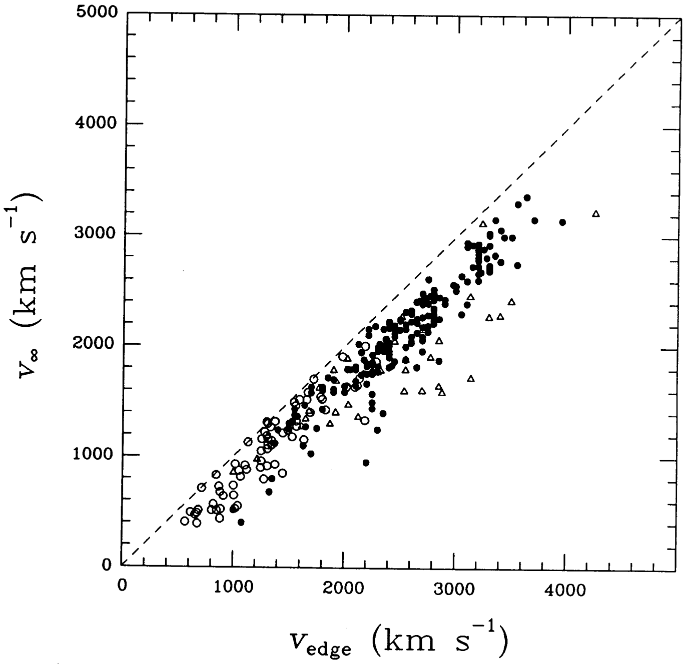

FIG. 5.—The terminal velocities of O (*filled circles*), B supergiant (*open circles*), and WR stars (*open triangles*) as a function of the maximum velocity observed in absorption in C IV, v_{edge}. The dashed line indicates the 1:1 relation for comparison.

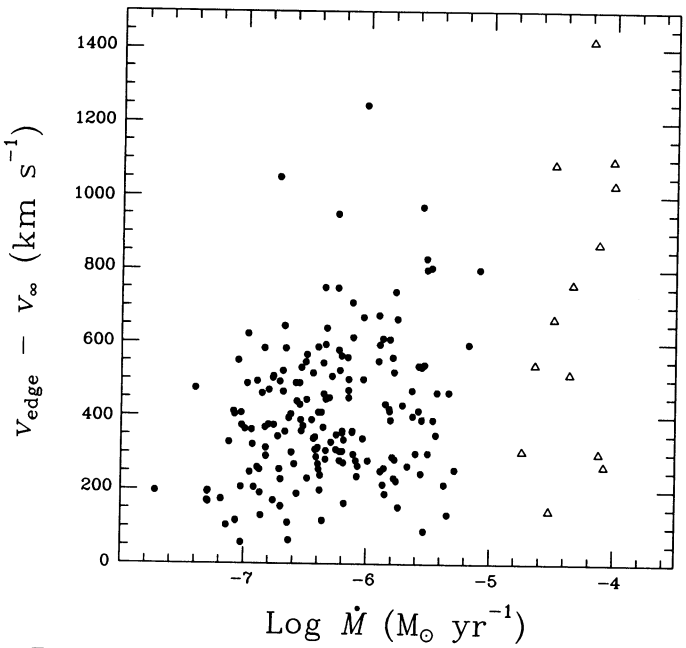

FIG. 6.—$v_{edge} - v_\infty$ as a function of mass-loss rate for O (*filled circles*) and WR (*open triangles*) stars.

that allowance for the high abundance of carbon in WC winds leads to an upward revision of the mass loss rates.

2. The ionization in WR winds has been predicted to decrease outward, such that the dominant ion at radio-emitting radii would be He^+ rather than He^{2+} (Schmutz and Hamann 1986; Hillier 1987*a*). This also leads to an upward revision of the mass-loss rates.

3. A reduction in the adopted wind terminal velocities (this paper) leads to a reduction in the derived mass-loss rates which is proportional to v_∞.

4. Very small (random) changes in the mass-loss rates are introduced by using distances from van der Hucht *et al.* (1988). (For HD 50896 we adopted $D = 2$ kpc, after Howarth and Phillips 1986).

The WR mass-loss rates listed in Table 5 have been derived using the formula of Wright and Barlow (1975) and the radio fluxes, or upper limits, measured by Abbott *et al.* (1986), Hogg (1982; for HD 214419), Becker and White (1985; the "low" state flux for HD 193793) and Hogg (1989; for HD 50896, 151932, 152270, 191765, and 192163). A temperature of 6000 K was adopted for the radio-emitting regions (Hogg 1985). For the WN stars, He^+ was assumed to be the dominant ion, except for the cases of HD 151932 and HD 193077, where we adopted $H^+/He^+ = 1$ and 1.6, respectively (Conti, Leep, and Perry 1983; Schmutz, Hamann, and Wessolowski 1988). For the WC stars we adopted $C^{2+}/He^+ = 0.3$ (Smith and Hummer 1988; Torres 1988). The mass loss rates listed in Table 5 assume the same wind terminal velocity in all directions from the WR star. Poe, Friend, and Cassinelli (1989) have proposed that WR stars may have lower terminal velocities and high densities in their equatorial zones, thereby reducing the mass-loss rates that should be derived from the observed radio fluxes.

Figure 6 shows the plot of $(v_{max} - v_\infty)$ versus log $\dot{M}$ for the O stars and WR stars in our sample. The O star mass-loss rates are those listed in Table 10 of Howarth and Prinja (1989), which include a statistical correction for the average effect of revised terminal velocities. A loose correlation ($r = 0.36$) between $\dot{M}$ and the excess absorption velocity ($v_{edge} - v_\infty$) is present in the data shown in Figure 6. To quantify this effect further, Table 6 lists the mean values of v_∞/v_{max} found for O V, O III, O I, B I, and WR stars. The mean value of v_∞/v_{edge} is found to decrease steadily from 0.88 for O V stars, 0.84 for O III and O II stars, through to 0.80 for O I and B I stars and 0.76 for WR stars. This is also a sequence of generally increasing C^{3+} column density. We interpret this trend in terms of two effects. First, among the O stars, the supergiants, which have higher mass-loss rates than the dwarfs or giants, tend to have lower terminal velocities (Table 3). If the amplitude of high-velocity perturbations in the wind was independent of the final terminal velocity reached, this might contribute part of the effect. Probably more important is the fact that the highest velocity material in an unstable radiatively driven wind is predicted to be extremely rarefied. In a low-density wind, such material would be unlikely to have enough optical depth to be seen in absorption, whereas a high mass-loss rate would lead to larger

TABLE 6

RATIO OF v_∞ TO v_{edge} AND v_{esc}

Spectral Type	Number	v_∞/v_{edge}	v_∞/v_{esc}
O I	39	0.80 ± 0.08	2.60 ± 0.38
O II	11	0.84 ± 0.06	2.75 ± 0.51
O III	35	0.84 ± 0.06	2.41 ± 0.47
O3 V–O7 V	45	0.87 ± 0.05	2.26 ± 0.37
O7.5 V–O9 V	19	0.89 ± 0.04	1.67 ± 0.44
ON	5	0.69 ± 0.15	1.38 ± 0.34
Ofp	5	0.70 ± 0.16	1.98 ± 0.52
B0 I–B3 I	65	0.80 ± 0.13	1.96 ± 0.60
WR	35	0.76 ± 0.12	...

NOTE.—Quoted errors are standard deviations.

absorption and a greater probability for the highest velocity material to be detectable.

We note that the present results do not significantly change the overall *slope* of the $\dot{M}$ versus L relation for OB stars, as determined by previous workers. Radio mass-loss rates (which scale as v_∞) have been obtained mainly for supergiants and so (from Table 6) should decrease by a mean factor of 0.80. UV-based mass loss rates (which scale as v_∞^2) have been derived mainly for samples of dwarfs and giants and so (from Table 6) should decrease by a mean factor of $(0.88)^2 = 0.77$. Thus the overall slope found for composite radio-UV samples should be unchanged, although the scale factor should be decreased by ~0.8. (This change in the scaling constant is already included in the mass-loss rates given by Howarth and Prinja 1989.)

Starting with Snow and Morton (1976) and Abbott (1978), the terminal wind velocities of OB stars have often been compared with their escape velocities, v_{esc}. In Figure 7 we plot the wind terminal velocities derived for the O stars in our sample against the escape velocities derived for them by Howarth and Prinja (1989); different symbols have been assigned to dwarfs, giants, and supergiants. The peculiar stars HD 37022 and HD 93521 have been excluded from this diagram.

The 70 B0–B3 supergiants in our sample are also plotted in Figure 7. Their escape velocities have been derived from the stellar parameters tabulated by Leitherer (1988) and are listed in Table 2 (where individual values of v_{esc} were not available, we adopted the mean value, indicated by parentheses, for the appropriate spectral subclass). Table 6 lists the mean values of (v_∞/v_{esc}) found for each of these groups. This ratio is found to increase from 1.7 for the late O dwarfs to 2.4 for the O giants and 2.6 for the O supergiants. The mean ratio found for all 151 O stars with assigned luminosity classes (but excluding Op, Oe, ON, and OC stars) is $v_\infty/v_{esc} = 2.36 \pm 0.51$. This compares with the ratio of 2.78 ± 0.36 derived for the 27 stars in their sample by Groenewegen, Lamers, and Pauldrach (1989). The latter authors have discussed possible reasons for the discrepancy between observed ratios of v_∞/v_{esc} and the value of 3.9 they obtain for radiation pressure–driven wind models.

The 249 stars plotted in Figure 7 (which excludes HD 93521 and HD 37022; § III*a*) yields a correlation coefficient of $r = 0.76$, while a least-squares fit to the data gives $v_\infty = (74 \pm 101) + (2.145 \pm 0.182)v_{esc}$ [or alternatively $v_{esc} = (333 \pm 29) + (0.266 \pm 0.015)\, v_\infty$]. The OB supergiants alone yield a correlation coefficient of $r = 0.83$.

Inspection of the mean values of v_∞/v_{max} listed in Table 6 reveals that the five Ofp stars in the sample have a low mean ratio of 0.70. Since, as discussed above, this ratio appears to decrease with increasing mass-loss rate, this behavior is consistent with the Ofp stars having higher mass-loss rates than other O stars. The mean value of v_∞/v_{esc} for the Ofp stars (1.98) is also significantly lower than found for the normal O stars. This may be due to the Ofp stars having already lost a large fraction of their original mass, with their current masses (and hence escape velocities) being overestimated by evolutionary track fitting. While there is a steady increase in v_∞/v_{esc} from 2.1 for the O V stars to 2.75 for the O II stars (Table 6), there is also a decrease in this quantity to 2.6 for the O I stars, suggesting the possibility that the higher mass-loss rates of this group again lead to lower masses, and therefore lower escape velocities, than predicted by the evolutionary tracks.

We find the interesting result that the five ON stars in our

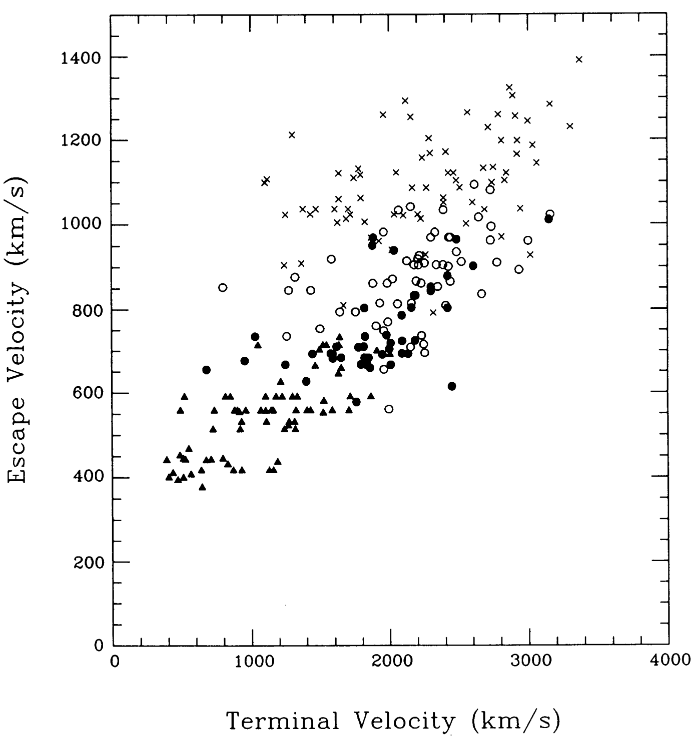

FIG. 7.—The photospheric escape velocity (see text for sources) versus the wind terminal velocity for B type supergiants (*filled triangles*), O type supergiants (*filled circles*), O type giants (*open circles*), and O type dwarfs (*crosses*).

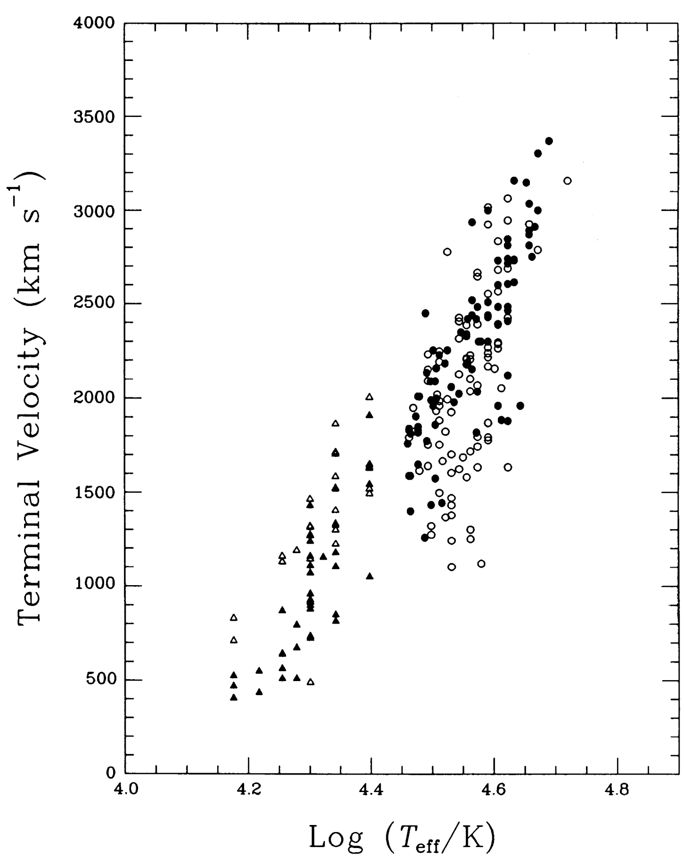

FIG. 8.—The terminal velocity as a function of effective temperature. The terminal velocities were derived from v_{black} and $v_{NAC} + \overline{HWHM}_{NAC}$ for O stars (*filled and open circles*, respectively) and B supergiants (*filled and open triangles*, respectively).

sample (three dwarfs and two supergiants) yield low mean values for both v_∞/v_{max} (0.69) and v_∞/v_{esc} (1.38; Table 6). The three ON dwarf stars all have spectral types between O7 and O9. The mean value of v_∞/v_{esc} for normal O dwarfs within this spectral type range is also low (1.67, Table 6), but the normal late O dwarfs have a mean value for v_∞/v_{max} of 0.89, significantly higher than found for the ON dwarfs. The ON stars might have physical parameters that are significantly different from those implied by their nominal spectral types. Schönberner *et al.* (1988) found that nitrogen was strongly enhanced in the atmospheres of a number of OBN main-sequence stars and discussed a variety of scenarios which might have led to this situation. For one of the stars, HD 14633 (ON8 V), their spectroscopically derived value of $\log g = 3.70$ is more like that expected for a giant than a main-sequence star and is 0.26 dex lower than the value derived from the parameters implied by its spectral type that are given by Howarth and Prinja (1989). If the mass and escape velocity of HD 14633 were correspondingly lowered, then the anomaly of its small value of v_∞/v_{esc} would disappear. Strong mixing, possibly rotationally induced, may lead to evolutionary tracks for ON stars near the main sequence quite unlike those for normal O stars (Maeder 1987), and hence the masses (and $\log g$ and v_{esc} values) estimated from evolutionary tracks could be in error. However, the reason for the low values found for the purely empirical ratio v_∞/v_{max} in the case of the ON stars is not obvious, unless these stars have much higher mass loss rates than hitherto suspected.

Finally, we note that although there is a good correlation ($r = 0.76$) between v_∞ and v_{esc} (Fig. 7), as predicted by radiation pressure driven–wind models, for the present sample an even better correlation ($r = 0.86$) exists between v_∞ and T_{eff}. Figure 8 shows a plot of terminal velocity versus T_{eff} for the O stars and B supergiants in our sample (we adopted the effective temperature scale of Howarth and Prinja 1989 for the O type stars, and the effective temperature scale of Barlow and Cohen 1977 for the B supergiants). Prinja (1990) has demonstrated that Be stars are also consistent with the trend shown in Figure 8. A similar trend to that shown in Figure 8 has been found for the central stars of planetary nebulae by Pauldrach *et al.* (1988). However, planetary nebula central stars exhibit a relatively narrow mass range ($0.60 \pm 0.02\ M_\odot$; Barlow 1989) and during their hydrogen-shell burning phase evolve to higher effective temperatures at constant luminosity, so the dependence of v_∞ upon T_{eff} is essentially the same as that upon v_{esc}. For the case of the OB stars plotted in Figure 8, a mass range as narrow as that found for planetary nebula central stars would be most unexpected.

We thank D. J. Stickland for information about the orbital phases corresponding to the *IUE* images of HD 190918 and HD 211853 and N. R. Walborn for recommendations in respect of spectral types.

REFERENCES

Abbott, D. C. 1978, *Ap. J.*, **225**, 893.
———. 1985, in *Progress in Stellar Line Formation Theory*, ed. J. E. Beckman and L. Crivellari (Dordrecht: Reidel), p. 279.
Abbott, D. C., Bieging, J. H., Churchwell, E., and Torres, A. V. 1986, *Ap. J.*, **303**, 239.
Barlow, M. J. 1989, in *IAU Symposium 131, Planetary Nebulae*, ed. S. Torres-Peimbert (Dordrecht: Kluwer), p. 319.
Barlow, M. J., and Cohen, M. 1977, *Ap. J.*, **213**, 737.
Barlow, M. J., Roche, P. F., and Aitken, D. K. 1988, *M.N.R.A.S.*, **232**, 821.
Becker, R. H., and White, R. L. 1985, *Ap. J.*, **297**, 649.
Castor, J. I., and Lamers, H. J. G. L. M. 1979, *Ap. J. Suppl.*, **39**, 481.
Conti, P. S., Leep, E. M., and Perry, D. N. 1983, *Ap. J.*, **268**, 228.
Fitzpatrick, E. L., Savage, B. D., and Sitko, M. L. 1982, *Ap. J.*, **256**, 578.
Groenewegen, M. A. T., Lamers, H. J. G. L. M., and Pauldrach, A. W. A. 1989, *Astr. Ap.*, **221**, 78.
Hamann, W.-R. 1980, *Astr. Ap.*, **84**, 342.
———. 1981, *Astr. Ap.*, **93**, 353.
Hamann, W.-R., Schmutz, W., and Wessolowski, U. 1988, *Astr. Ap.*, **194**, 190.
Heap, S. R. 1982, in *Advances in Ultraviolet Astronomy* (NASA CP-2238), p. 562.
Heck, A., Egnet, D., Jaschek, M., and Jaschek, C. 1984, *IUE Low Dispersion Spectral Atlas* (ESA SP-1052).
Henrichs, H. F., Kaper, L., and Zwarthoed, G. A. A. 1988, in *A Decade of UV Astronomy with the IUE Satellite* (ESA SP-281), Vol. **2**, p. 145.
Hillier, D. J. 1987*a*, *Ap. J. Suppl.*, **63**, 947.
———. 1987*b*, *Ap. J. Suppl.*, **63**, 965.
———. 1989, *Ap. J.*, **347**, 392.
Hiltner, W. A. 1956, *Ap. J. Suppl.*, **2**, 389.
Hogg, D. E. 1982, in *IAU Symposium 99, Wolf-Rayet Stars: Observations, Physics, Evolution*, ed. C. W. H. de Loore and A. J. Willis (Dordrecht: Reidel), p. 221.
———. 1985, in *Radio Stars*, ed. R. M. Hjellming and D. M. Gibson (Dordrecht: Reidel), p. 117.
———. 1989, *Pub. A.S.P.*, **98**, 282.
Howarth, I. D. 1984*a*, *M.N.R.A.S.*, **206**, 625.
———. 1984*b*, *M.N.R.A.S.*, **211**, 167.
Howarth, I. D., and Phillips, A. P. 1986, *M.N.R.A.S.*, **222**, 809.
Howarth, I. D., and Prinja, R. K. 1989, *Ap. J. Suppl.*, **69**, 527.
Koenigsberger, G., and Auer, L. H. 1987, *Rev. Mexicana Astr. Af.*, **14**, 271.
Kondo, Y., Feibelman, W. A., and West, D. K. 1982, *Ap. J.*, **252**, 208.
Lamers, H. J. G. L. M., Gathier, R., and Snow, T. P. 1982, *Ap. J.*, **258**, 186.
Leitherer, C. 1988, *Ap. J.*, **326**, 356.
Lesh, J. R. 1968, *Ap. J. Suppl.*, **16**, 371.
Lucy, L. B. 1982, *Ap. J.*, **255**, 278.
———. 1983, *Ap. J.*, **274**, 372.
Maeder, A. 1987, *Astr. Ap.*, **178**, 159.
Morgan, W. W., Code, A. D., and Whitford, A. E. 1956, *Ap. J. Suppl.*, **2**, 41.
Morton, D. C. 1976, *Ap. J.*, **203**, 386.
Owocki, S., Castor, J. I., and Rybicki, G. B. 1988, *Ap. J.*, **335**, 914 (OCR).
Pauldrach, A., Puls, J., Kudritzki, R. P., Mendez, R. H., and Heap, S. R. 1988, *Astr. Ap.*, **207**, 123.
Poe, C. H., Friend, D. B., and Cassinelli, J. P. 1989, *Ap. J.*, **337**, 888.
Prinja, R. K. 1988, *M.N.R.A.S.*, **231**, 21p.
———. 1989, *M.N.R.A.S.*, **241**, 721.
———. 1990, *Astr. Ap.*, **232**, 119.
Prinja, R. K., and Howarth, I. D. 1986, *Ap. J. Suppl.*, **61**, 357.
———. 1988, *M.N.R.A.S.*, **233**, 123.
Prinja, R. K., Howarth, I. D., and Henrichs, H. F. 1987, *Ap. J.*, **317**, 389.
St-Louis, N., Willis, A. J., and Smith, L. J. 1988, in *A Decade of UV Astronomy with the IUE Satellite* (ESA SP-281), **2**, p. 125.
Schmutz, W., and Hamann, W.-R. 1986, *Astr. Ap.*, **166**, L11.
Schmutz, W., Hamann, W.-R., and Wessolowski, U. 1989, *Astr. Ap.*, **210**, 236.
Schoenberner, D., Herrero, A., Becker, S., Eber, F., Butler, K., Kudritzki, R. P., and Simon, K. P. 1988, *Astr. Ap.*, **197**, 209.
Shore, S. N., and Brown, D. N. 1988, *Ap. J.*, **334**, 1021.
Smith, L. F., and Hummer, D. G. 1988, *M.N.R.A.S.*, **230**, 511.
Snow, T. P. 1977, *Ap. J.*, **217**, 760.
Snow, T. P., and Morton, D. C. 1976, *Ap. J. Suppl.*, **32**, 429.
Stickland, D. S. 1989, *Observatory*, **109**, 74.
Torres, A. V. 1988, *Ap. J.*, **325**, 759.
Torres, A. V., Conti, P. S., and Massey, P. 1986, *Ap. J.*, **300**, 379.
Uesugi, A., and Fukuda, I. 1982, *Revised Catalogue of Stellar Rotational Velocities* (Kyoto: Department of Astronomy, Kyoto University).
van der Hucht, K. A., Cassinelli, J. P., and Williams, P. M. 1986, *Astr. Ap.*, **168**, 111.
van der Hucht, K. A., Conti, P. S., Lundstrom, I., and Stenholm, B. 1981, *Space Sci. Rev.*, **28**, 227.
van der Hucht, K. A., Hidayat, B., Admiranto, A. G., Supelli, K. R., and Doom, C. 1988, *Astr. Ap.*, **199**, 217.
van Genderen, A. M., *et al.* 1988, *Astr. Ap. Suppl.*, **74**, 467.
Walborn, N. R., and Nichols-Bohlin, J. 1987, *Pub. A.S.P.*, **99**, 611.
Williams, P. M., and Eenens, P. R. J. 1989, *M.N.R.A.S.*, **240**, 445.
Willis, A. J. 1982, *M.N.R.A.S.*, **198**, 897.
Wright, A. E., and Barlow, M. J. 1975, *M.N.R.A.S.*, **170**, 41.

M. J. Barlow, I. D. Howarth, and R. K. Prinja: Department of Physics and Astronomy, University College London, G er Street, London WC1E 6BT, England, UK
[SPAN: 19457::ZUVAD::MJB, IDH, RKP;
Bitnet: MJB, IDH, RKP@STAR.UCL.AC.UK]